

Increased K⁺ Efflux and Apoptosis Induced by the Potassium Channel Modulatory Protein KChAP/PIAS3 β in Prostate Cancer Cells*

Received for publication, February 9, 2002
Published, JBC Papers in Press, March 4, 2002, DOI 10.1074/jbc.M201689200

Barbara A. Wible \ddagger §, Liming Wang, Yuri A. Kuryshev, Aruna Basu, Subrata Haldar \parallel ||, and Arthur M. Brown**

From the Rammelkamp Center for Education and Research, MetroHealth Campus, and the Departments of \ddagger Biochemistry, **Physiology and Biophysics, \parallel Pharmacology, and $\parallel\parallel$ Ireland Cancer Center, Case Western Reserve University, Cleveland, Ohio 44109

K⁺ channel-associated protein/protein inhibitor of activated STAT (KChAP/PIAS3 β) is a potassium (K⁺) channel modulatory protein that boosts protein expression of a subset of K⁺ channels and increases currents without affecting gating. Since increased K⁺ efflux is an early event in apoptosis, we speculated that KChAP might induce apoptosis through its up-regulation of K⁺ channel expression. KChAP belongs to the protein inhibitor of activated STAT family, members of which also interact with a variety of transcription factors including the proapoptotic protein, p53. Here we report that KChAP induces apoptosis in the prostate cancer cell line, LNCaP, which expresses both K⁺ currents and wild-type p53. Infection with a recombinant adenovirus encoding KChAP (Ad/KChAP) increases K⁺ efflux and reduces cell size as expected for an apoptotic volume decrease. The apoptosis inducer, staurosporine, increases endogenous KChAP levels, and LNCaP cells, 2 days after Ad/KChAP infection, show increased sensitivity to staurosporine. KChAP increases p53 levels and stimulates phosphorylation of p53 residue serine 15. Consistent with activation of p53 as a transcription factor, p21 levels are increased in infected cells. Wild-type p53 is not essential for induction of apoptosis by KChAP, however, since KChAP also induces apoptosis in DU145 cells, a prostate cancer cell line with mutant p53. Consistent with its proapoptotic properties, KChAP prevents growth of DU145 and LNCaP tumor xenografts in nude mice, indicating that infection with Ad/KChAP might represent a novel method of cancer treatment.

Apoptosis, or programmed cell death, is a multistage process starting with cell shrinkage followed by chromatin condensation, caspase activation, and cellular fragmentation with subsequent removal of apoptotic bodies by neighboring cells. Early cell shrinkage is due in part to increased K⁺ efflux (reviewed in Ref. 1). Loss of K⁺ during apoptosis is not an epiphenomenon but is critical to its progression. Block of K⁺ currents by channel-specific drugs or high extracellular K⁺ prevents apoptosis

(2–5). Importantly, caspase activation, considered the point of no return in apoptosis, only occurs after cellular K⁺ loss (6). Despite the importance of this process, virtually nothing is known about the mechanisms generating increased K⁺ efflux. Here, we investigate the link between the actions of a K⁺ channel modulatory protein, KChAP/PIAS3 β ,¹ and apoptosis in tumor cells.

KChAP/PIAS3 β is a K⁺ channel modulatory protein that exhibits “chaperone-like” behavior toward a subset of K⁺ channels (7–9). KChAP, a soluble protein, binds transiently to the cytoplasmic NH₂ termini of its target channels and increases channel expression in a transcription-independent manner. Both total channel protein and surface expression are increased in response to KChAP. We hypothesized that the increased K⁺ channel expression conferred by KChAP might be associated with apoptosis.

In addition to K⁺ channels, KChAP/PIAS3 β interacts with other binding partners, most notably a variety of transcription factors. KChAP belongs to the protein inhibitor of activated STAT (PIAS) gene family. There are four mammalian members of this family: 1) KChAP (7)/PIAS3 (10), 2) Gu-binding protein (11)/PIAS1 (12), 3) androgen receptor-interacting protein 3 (13)/PIAS α (12) and Miz1 (14)/PIAS β (12), and 4) PIASy (12, 15). The multiple names of most of these genes reflect their independent cloning as binding partners of different proteins. KChAP and PIAS3 are alternatively spliced products of a single gene; in KChAP, a small intron in the NH₂-terminal coding region is retained, generating an in-frame insertion of 39 amino acids. We refer to KChAP as PIAS3 β to distinguish it from the original mouse PIAS3 clone (10), which we refer to as PIAS3 α . Mouse PIAS3 (PIAS3 α) binds to activated STAT3 and prevents its attachment to DNA (10). PIAS proteins may also act as coregulators of steroid hormone transcription factors including androgen, glucocorticoid, and progesterone receptors (13, 16–18). PIASy (15) and PIAS1 (19) have been found to interact with p53 and differentially affect its transcriptional activity. PIASy blocked the ability of p53 to transcribe its target gene, p21 (15), whereas PIAS1 activated p53-mediated gene expression including p21 (19).

The interactions of PIAS proteins (KChAP/PIAS3 β) with K⁺ channels and p53 were the starting point of the present exper-

* This work was supported by National Institutes of Health (NIH) Grant HL60759 (to B. A. W.) and NIH Grants HL-55404, HL-36930, HL-61642, and 3DK54178 (to A. M. B.). The costs of publication of this article were defrayed in part by the payment of page charges. This article must therefore be hereby marked “advertisement” in accordance with 18 U.S.C. Section 1734 solely to indicate this fact.

§ To whom correspondence should be addressed: Rammelkamp Center for Education and Research, MetroHealth Campus, Case Western Reserve University, 2500 MetroHealth Dr., Cleveland, OH 44109. Tel.: 216-778-8984; Fax: 216-778-8282; E-mail: bwible@metrohealth.org.

¹ The abbreviations used are: KChAP, K⁺ channel-associated protein; PIAS, protein inhibitor of activated STAT; STAT, signal transducers and activators of transcription; STS, staurosporine; Ad, adenovirus; GFP, green fluorescent protein; PBS, phosphate-buffered saline; MOI, multiplicity of infection; PI, propidium iodide; potassium-binding benzofuran isophthalate; TUNEL, terminal deoxynucleotidyl transferase-mediated dUTP nick end labeling; PARP, poly(ADP-ribose) polymerase.

iments. We hypothesized that KChAP might contribute to apoptosis, on the one hand by increasing K^+ efflux in association with apoptotic cell volume decrease and, on the other, by activating p53. To test this hypothesis, a nonreplicating, recombinant adenovirus containing KChAP cDNA was constructed (AdKChAP) for infection of LNCaP cells, selected because they express both K^+ currents and wild type p53. We found that overexpression of KChAP increased K^+ efflux, reduced LNCaP cell volume, and induced apoptosis as evidenced by positive COMET assay and PARP cleavage. KChAP interacted with the p53 tetramerization domain in yeast two-hybrid studies, and total p53 as well as the phosphoserine 15 form were increased in Ad/KChAP-infected LNCaP cells. Consistent with activation of p53 transcription factor activity, p21, a G_1 cell cycle arrest protein, was up-regulated in these cells. Ad/KChAP also produced apoptosis in another prostate cancer cell line, DU145 cells, which contain mutant p53. Given its proapoptotic effects independent of p53 status, we proposed that KChAP might act as a tumor suppressor, and we found that injection of Ad/KChAP into LNCaP and DU145 tumor xenografts in nude mice produced apoptosis and suppression of tumor growth.

EXPERIMENTAL PROCEDURES

Cell Culture and Adenovirus Infection

LNCaP, DU145, and Jurkat cells were obtained from the American Type Culture collection. LNCaP and Jurkat cells were maintained in RPMI medium with 10% fetal bovine serum, while DU145 cells were propagated in Dulbecco's modified Eagle's medium plus 10% fetal bovine serum. All media also contained 100 units/ml penicillin and 100 μ g/ml streptomycin. In the LNCaP experiments with high extracellular K^+ in the medium, RPMI medium was assembled from the individual components as outlined by Invitrogen so that we could adjust the $[K^+]$. The total amount of K^+ plus Na^+ in the media was kept constant at 108.4 mM so that when $[K^+]$ was elevated, $[Na^+]$ was correspondingly decreased. Staurosporine (STS) was from Sigma, and a 1 mM stock solution was prepared in Me_2SO and stored at $-20^\circ C$. A final concentration of 1 μ M was used to induce apoptosis.

A replication-defective, recombinant KChAP/adenovirus was constructed as follows. Full-length KChAP cDNA was subcloned in the vector, pShuttle-CMV, and sent to Q-Biogene (Montreal, Quebec, Canada) for adenovirus construction and purification. Expression of KChAP from the recombinant adenovirus, Ad/KChAP, was verified by Western blotting lysates of infected cells with a KChAP-specific antibody, 088, which recognizes only overexpressed KChAP (see details below). Recombinant Ad/GFP and Ad/LacZ were purchased from Q-Biogene. Viral infections were performed by diluting the virus to the appropriate concentration in standard medium and overlaying the cells (1 ml/35-mm dish). The medium was not changed before the cells were harvested.

Antibodies and Western Blotting

We used two KChAP antibodies in this study, both of which were generated in our laboratory. 899 was raised against a bacterial fusion protein that consisted of the COOH-terminal 169 amino acids of KChAP (5). It recognizes both endogenous and overexpressed KChAP. 088 was raised against a peptide in the NH_2 terminus of KChAP that is not present in PIAS3 (SPSPLASIPPTLLTPGTLLGPKREVDMMH), hence the PIAS3 α and PIAS3 β /KChAP nomenclature used here. 088 recognizes overexpressed but not endogenous KChAP. Affinity-purified antibodies were used in Western blotting. Other antibodies used for Western blotting to detect the following proteins were obtained from commercial sources: p53 (DO-1; Santa Cruz Biotechnology, Inc., Santa Cruz, CA); STAT1, STAT3, and cyclins A, B, and D3 (Transduction Laboratories, Lexington, KY); actin (clone AC-40; Sigma); phospho-p53 (Ser¹⁵) (Cell Signaling Technology, Inc., Beverly, MA); PARP (we used two antibodies interchangeably that recognize both intact and cleaved PARP, one from Cell Signaling Inc. and one from BD PharMingen (San Diego, CA)); monoclonal Rb (BD PharMingen); and p21 (WAF1 Ab1; Oncogene Research Products (Boston, MA)).

Cells were lysed in a buffer consisting of 1% Triton X-100, 150 mM NaCl, 50 mM Tris, 1 mM EDTA, pH 7.5 containing freshly added protease inhibitors (Complete; Roche Molecular Biochemicals) and the phosphatase inhibitors sodium fluoride (50 mM) and sodium orthovanadate (1 mM) for 30 min on ice. Insoluble debris was pelleted at 20,800 \times

g for 10 min at $4^\circ C$. Lysate protein concentrations were determined by the BCA method (Pierce), and aliquots were boiled in a reducing SDS sample buffer to denature protein. SDS-PAGE gels were blotted to polyvinylidene difluoride membranes using a semidry blotting apparatus. Blots were blocked overnight in 5% milk (Bio-Rad) in PBS-T (PBS plus 0.1% Tween 20) at $4^\circ C$. Primary antibodies diluted in blocking buffer were incubated with the blots for 1 h at room temperature. Blots were washed with PBS-T and incubated with horseradish peroxidase-conjugated secondary antibodies (Amersham Biosciences) in blocking buffer for 1 h at room temperature. Blots were developed with the ECL-Plus kit (Amersham Biosciences).

Yeast Two-hybrid Assay

Full-length KChAP (residues 1–619) in the GAL4 activation domain vector, pGAD424, was used as described (5). Murine p53 (residues 90–390) in a GAL4 DNA binding domain vector was from the CLONTECH Matchmaker yeast two-hybrid kit. The murine p53 carboxyl terminus (residues 290–390) and subfragments (Phe³²⁴–Thr³⁵²) and (Phe³³⁴–Thr³⁵²) with *Eco*RI and *Sal*I sites incorporated at the 5' and 3'-ends of the fragments, respectively, were generated by PCR. PCR products were subcloned using TOPO cloning (Invitrogen; Carlsbad, CA) and sequenced before cloning in frame into pGBT9 and pGAD424. Yeast strain *Y190* was transformed with combinations of pGBT9 and pGAD424 plasmids, and interaction was determined by β -galactosidase filter assays as previously described (7).

COMET Assay

DNA degradation was assayed in cells overexpressing Ad/KChAP or Ad/LacZ using the kit from Trevigen. Briefly, 10^6 cells/ml were mixed with molten low melting agarose at a ratio of 1:10. Immediately, 50 μ l of this mixture was spread onto slides. Slides were immersed in pre-chilled lysis solution at $4^\circ C$ for 30 min. After a brief rinse in $1\times$ TBE, the slides were subjected to horizontal electrophoresis at 1 V/cm (measured electrode to electrode) for 11 min. The slides were then put in ice-cold methanol for 5 min followed by a 5-min incubation at room temperature in ethanol. After drying, the slides were stained with SYBR green for epifluorescence microscopy.

Rb⁺ Flux

LNCaP cells were plated in six-well tissue culture dishes at 250,000 cells/well. On the following day, cells were infected with either Ad/GFP or Ad/KChAP (multiplicity of infection (MOI) = 100). Rb⁺ fluxes were measured 24 h after infection using the nonradioactive method of Terstappen (20). To load Rb⁺, cells were incubated for 4 h ($37^\circ C$) in a modified Tyrode's solution containing 5 mM RbCl, 145 mM NaCl, 1.8 mM CaCl₂, 1 mM MgCl₂, 10 mM HEPES, 10 mM glucose (pH 7.4 at $37^\circ C$), and 10% fetal bovine serum. The cells were then washed three times with Rb⁺-free PBS and incubated for 10 min at room temperature in 1 ml of normal Tyrode's solution. The supernatant containing released Rb⁺ was collected, and the cells were lysed in 1 ml of PBS containing 1% Triton X-100 to measure Rb⁺ remaining in the cells. Samples were diluted (1:4) with ionization buffer (PBS containing 2.5% HNO₃), and Rb⁺ content was determined using flame atomic absorption spectrometry at 780 nm (PerkinElmer Life Sciences model 3100). A calibration curve was constructed to determine Rb⁺ concentrations. Relative Rb⁺ efflux was calculated as the amount of Rb⁺ in the supernatant divided by total Rb⁺ (supernatant plus cell lysate).

Flow Cytometric Analysis

K⁺ Content—At 72 h postinfection with either Ad/GFP or Ad/KChAP (MOI = 100), LNCaP cells were collected by trypsin treatment and washed in PBS. The K^+ -sensitive dye, potassium-binding benzofuran isophthalate (PBFI) (Molecular Probes, Inc., Eugene, OR) was dissolved in Pluronic F-127 (Molecular Probes) and incubated with the cells in standard medium at a final concentration of 5 μ M for 1 h at $37^\circ C$. The cells were then chilled on ice, and propidium iodide (5 μ g/ml) was added. Flow cytometry was performed with a Becton Dickinson FACS Vantage machine. Ten thousand cells from each treatment group were analyzed. Excitation of PBFI was at 340 nm, and emission was captured at 425 nm. Propidium iodide was excited by a 488-nm argon laser at the same time.

DNA Content—For analysis of DNA content, cells were trypsinized either 24 or 72 h postinfection as described above, washed with PBS, and fixed in cold 70% ethanol for at least 8 h at $-20^\circ C$. After washing in PBS, propidium iodide (5 μ g/ml) was added. Ten thousand cells were examined by flow cytometry for each sample using a Becton Dickinson FACScan (excitation at 488 nm).

Tumor Production and Adenovirus Injection in Nude Mice

Tumor cells (DU145 or LNCaP; 2×10^6 cells/injection site) were suspended in serum-free Dulbecco's modified Eagle's medium, mixed with an equal volume of cold Matrigel on ice, and injected subcutaneously into both flanks of 8–9-week-old female BALB/c nude mice. Tumor growth was monitored using calipers every 2–3 days. Tumor volume was calculated as $(L \times W^2)/2$, where L represents length and W is width in millimeters. When tumors reached an average size of 50–60 mm³ (about 2 weeks for DU145 and 5 weeks for LNCaP), mice were divided into three treatment groups: 1) PBS, 2) Ad/GFP, and 3) Ad/KChAP. Both tumors on an individual mouse received the same treatment. Ad/GFP and Ad/KChAP were diluted in sterile PBS to 5×10^8 plaque-forming units/ μ l. Injections (1μ l/mm³ of tumor) were delivered directly into the tumors every 2–3 days for a total of three injections per week. Assuming 10^6 cells per mm³ of tumor, about 500 plaque-forming units of virus per tumor cell was injected at 48–72 h intervals. Mice were sacrificed by cervical dislocation 48 h after the final injection, and tumors were dissected and frozen in liquid nitrogen. During the experiments, the animals were housed and handled in accordance with the National Institutes of Health guidelines.

Immunohistochemistry and Terminal Deoxynucleotidyl Transferase-mediated dUTP Nick End Labeling (TUNEL) Assay of Tumor Sections

Eight-micron sections were prepared from frozen tumors dissected from the three treatment groups (PBS, Ad/GFP, and Ad/KChAP), mounted, and fixed on glass slides. Overexpressed KChAP was detected by incubating sections with the 088 antibody (1:100 dilution in 0.2% gelatin plus 0.5% bovine serum albumin/PBS) for 2 h at room temperature, washing with PBS, and incubating with biotinylated anti-rabbit secondary antibody (1:200) for 1 h at room temperature. Color development was done with the ABC and DAB kits from Vector Laboratories following their instructions. Apoptosis of cells in tumors subjected to different treatments was determined by the TUNEL assays using the Apo-Tag kit (Oncor, Inc.), following the manufacturer's instructions.

RESULTS

KChAP Increases K⁺ Efflux in LNCaP Cells—We originally identified KChAP as a potassium channel regulatory protein that acts to increase K⁺ channel expression in a “chaperone-like” fashion in heterologous expression systems. Since one of the first events in apoptosis is cell shrinkage mediated, in part, by efflux of potassium, we speculated that KChAP may play a role in increasing K⁺ currents and thus promote apoptosis. We chose to work with several well studied cancer cell lines, since the induction of apoptosis in these cells by a novel protein might lead to new therapeutic strategies. To determine how KChAP affected K⁺ currents in these cells, we first overexpressed KChAP in the prostate cancer line LNCaP through the use of a recombinant adenovirus construct. Infection of LNCaP cells with adenovirus overexpressing GFP (Ad/GFP), at an MOI of 100, resulted in greater than 95% of the cells expressing GFP (data not shown). To examine K⁺ flux, LNCaP cells were infected with either Ad/GFP or Ad/KChAP (MOI of 100) for 24 h, after which they were loaded with the potassium surrogate rubidium (Rb⁺) and assayed for Rb⁺ release by flame atomic absorption spectroscopy. As shown in Fig. 1A, KChAP-overexpressing cells showed a significant increase (about 20%) in the fraction of Rb⁺ released compared with cells infected with a GFP virus.

We measured the relative amount of K⁺ in Ad/KChAP-infected cells at later times after infection using flow cytometry with the potassium-sensitive dye, PBFI. LNCaP cells were harvested 72 h postinfection with Ad/KChAP (MOI = 100). Uninfected cells were used for comparison, since the expression of GFP would have interfered with the detection of the dye. In Fig. 1B, the amount of PBFI fluorescence reflecting intracellular K⁺ was plotted against propidium iodide (PI) fluorescence. Cells with high PI intensity (R1 section) were dead cells and thus not analyzed further. In cells with low PI fluorescence (live cells, sections R2 and R3), there was a clear shift of the

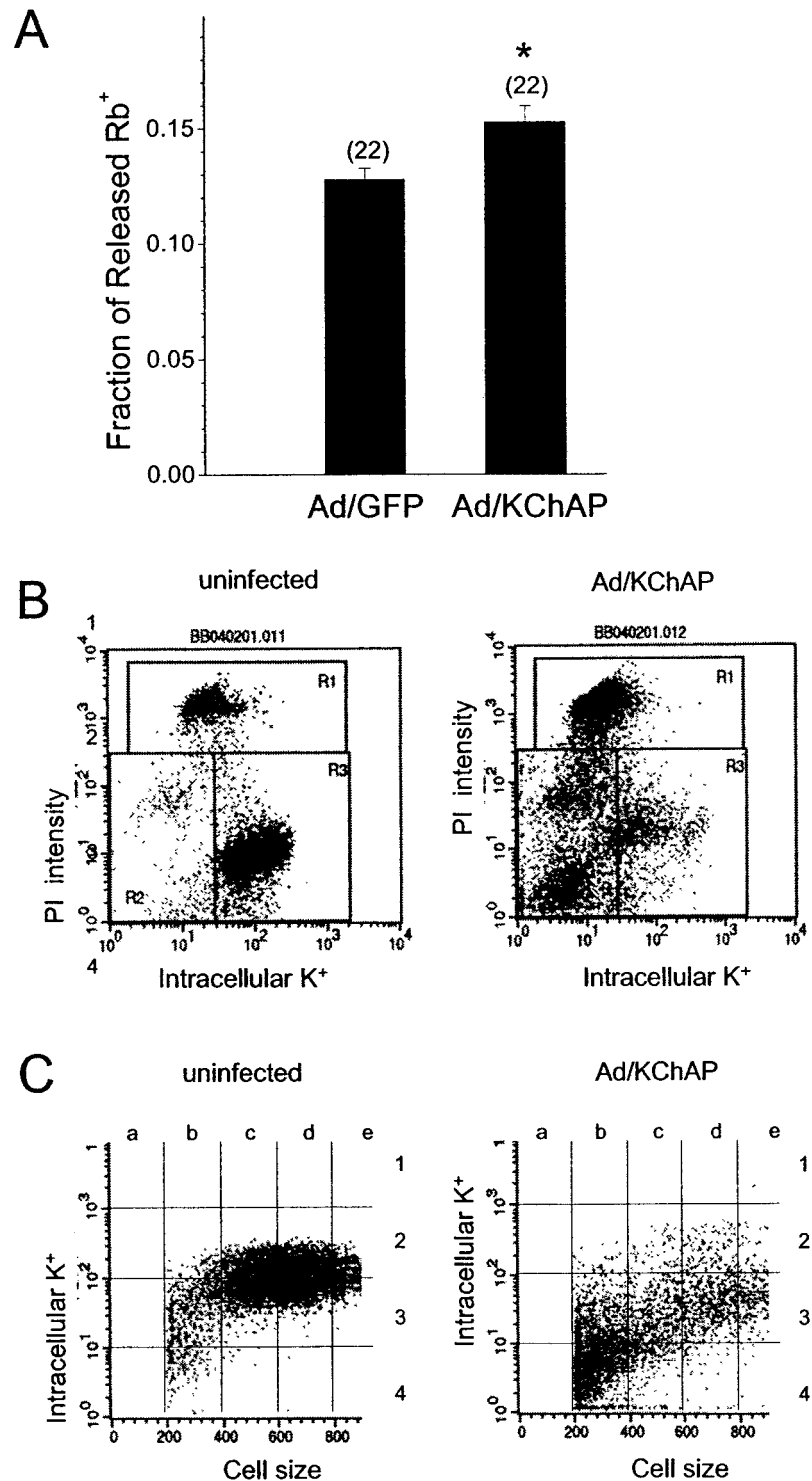
population to lower intracellular K⁺ levels. Since we are measuring total K⁺ and not K⁺ concentration, this decrease in K⁺ may reflect cell shrinkage. When the cells in R2 and R3 were replotted to examine cell size (reflected in the forward scatter values collected from the flow cytometer) versus intracellular K⁺ (Fig. 1C), we found that this is the case. In KChAP-infected cells, there was a dramatic decrease in average cell size that paralleled the decrease in intracellular K⁺. Thus, KChAP stimulated release of K⁺ from cells when measured 24 h after introduction of the Ad/KChAP virus and produced a significant decrease in cell size when assessed 72 h postinfection. From the data in Fig. 1C, it also appeared that the concentration of K⁺ was decreased in apoptotic, Ad/KChAP-infected cells. For example, the smallest uninfected cells fell into sector b3 (<400 cell size units), whereas the majority of the smallest KChAP-infected cells fell into sector b4 (Fig. 1C).

KChAP Sensitizes Cells to Apoptotic Stimuli—Since KChAP increases K⁺ efflux and shrinks LNCaP cells, we hypothesized that if KChAP was a proapoptotic protein, overexpression in LNCaP cells should sensitize the cells to apoptosis induced by STS. LNCaP cells 2 days postinfection (MOI of 100) with either Ad/GFP or Ad/KChAP were treated with STS and lysed, and apoptosis was assessed by PARP cleavage on Western blots. As shown in Fig. 2A, no PARP cleavage was detected in cells overexpressing either GFP or KChAP 2 days after infection. PARP cleavage was detected as early as 2 h after the addition of STS (1μ M) in KChAP-expressing cells and was about 50% complete at 6 h. This is in contrast to GFP-expressing cells in which PARP cleavage was not detectable at all until 6 h of STS treatment. KChAP expression was examined with the 899 antibody, which detects both endogenous and overexpressed KChAP. Overexpressed KChAP migrates at the same position as the endogenous 68-kDa doublet and largely disappears as PARP cleavage progresses. Thus, KChAP makes LNCaP cells more sensitive to STS-induced apoptosis.

In the course of these experiments, we observed an increase in the amount of endogenous KChAP detected in cells exposed to STS. Fig. 2B shows Western blots of endogenous KChAP from both LNCaP and Jurkat cells treated for various lengths of time with 1μ M STS. Multiple bands are detected in both cell lysates with the KChAP 899 antibody: a 68-kDa doublet that is close to the predicted molecular weight of KChAP and PIAS3 and an upper band of about 85 kDa. Fig. 2B shows that the signal of the 68-kDa doublet obtained with the KChAP 899 antibody is increased as early as 1 h after the addition of STS. The signal then drops to control levels or lower after about 6 h in LNCaP cells and around 4–6 h in Jurkat cells. This peak in immunoreactivity largely precedes detection of PARP cleavage, a marker for apoptosis. Once significant PARP cleavage is detected, much less KChAP is detected by Western blotting. There was no change in the 85-kDa band. This phenomenon is not limited to STS, since the same pattern was also obtained with the apoptosis-inducing drug camptothecin (data not shown). Whether the increased signal on Western blots is due to increased KChAP protein levels or posttranslational modification of the protein to make antibody binding more accessible is not yet known. However, this pattern is consistent with a proapoptotic protein that is up-regulated or activated early after the apoptotic stimulus.

KChAP Alone Induces Apoptosis in LNCaP Cells—The data in Fig. 2 are consistent with KChAP as a proapoptotic protein, and in Fig. 1, we showed that KChAP promotes K⁺ loss and cell shrinkage. Is KChAP overexpression alone sufficient to induce apoptosis? In Fig. 2A, we saw no PARP cleavage in Ad/KChAP-infected LNCaP cells at 2 days postinfection in the absence of STS. When infected LNCaP cultures were examined microscop-

FIG. 1. Increased K⁺ loss from LNCaP cells overexpressing KChAP. *A*, overexpression of KChAP in LNCaP cells for 24 h results in increased basal Rb⁺ efflux compared with control cells overexpressing GFP. The number of 35-mm wells of cells examined is indicated above the bars. *, significant difference compared with the control ($p < 0.005$). *B*, flow cytometry of LNCaP cells 72 h after Ad/KChAP infection. In unfixed cells, intracellular K⁺ was measured with the K⁺ binding dye, PBFI, and plotted versus PI fluorescence (to distinguish between live and dead cells). Cells in R1 (high PI fluorescence) are classified as dead cells. Most uninfected control cells fall into R3 (low PI, normal K⁺), whereas Ad/KChAP-infected cells show a major shift of the population to R2 (low PI, decreased K⁺). *C*, comparison of intracellular K⁺ with cell size in control and Ad/KChAP-infected cells. Dead cells in R1 were removed from analysis, and those in R2 and R3 were replotted to evaluate K⁺ as a function of cell size. Cell size was estimated by forward scatter. Decreased intracellular K⁺ in KChAP-overexpressing cells correlated with cell shrinkage. A grid was placed over each panel to emphasize the decreased intracellular K⁺ seen in KChAP-infected cells compared with uninfected cells of the same size.

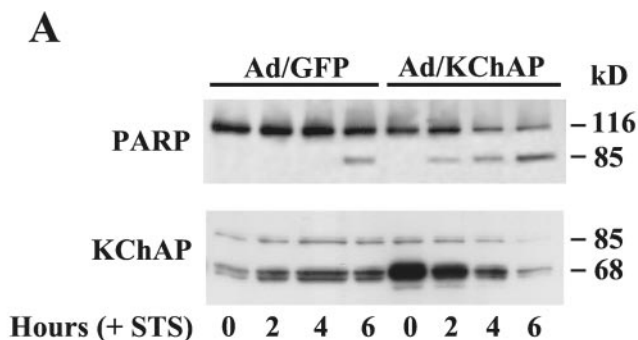


ically at later times after infection, however, we observed that many of the cells had become detached from the culture dish, consistent with cell death. We assayed for apoptosis in cells 3 days after infection using the COMET assay to detect DNA degradation. In these experiments, control infections were done with Ad/LacZ to prevent interference of GFP with the COMET assay. Fig. 3 shows the results of four independent infections. The top panel shows a typical field of nuclei assayed from cells infected with Ad/LacZ (left) or Ad/KChAP (right). Quantitation of the number of COMET-positive cells is presented in the table below. A substantial increase (about 25-fold) in the number of cells with degraded DNA is observed in cells overexpressing

KChAP compared with LacZ (an average of 24.4% COMET-positive versus 0.8%, respectively).

In addition to the COMET assay, we also examined PARP cleavage in cells 3 days postinfection (Fig. 3, bottom panel). Lysates from LNCaP cells infected with either Ad/LacZ or Ad/KChAP at an MOI of 100 were probed with anti-PARP antibody on Western blots. Lysates from three different batches of infected cells showed detectable PARP cleavage coincident with the expression of KChAP. The KChAP antibody 088, which only detects overexpressed KChAP, was used to verify Ad/KChAP viral infection. Thus, overexpression of KChAP is able to trigger apoptosis in LNCaP cells, with both

FIG. 2. KChAP appears as a pro-apoptotic protein. *A*, overexpression of KChAP via an adenovirus/KChAP construct (Ad/KChAP) accelerates the rate at which LNCaP cells undergo STS-induced apoptosis. Apoptosis in LNCaP cells infected with either Ad/GFP or Ad/KChAP (MOI of 100; greater than 95% of cells infected) was monitored by examining PARP cleavage on Western blots. KChAP, both endogenous and overexpressed, was detected with the KChAP antibody (899). *B*, KChAP (68 kDa) immunoreactivity increases in LNCaP and Jurkat T-cells treated with STS (1 μ M). Western blot analysis of KChAP and PARP expression in lysates of LNCaP and Jurkat cells shows increased reactivity of the 68-kDa band with the KChAP antibody after treatment with STS. Increased immunoreactivity is maintained until significant PARP cleavage is detected, after which the signal drops to control levels or below.



B

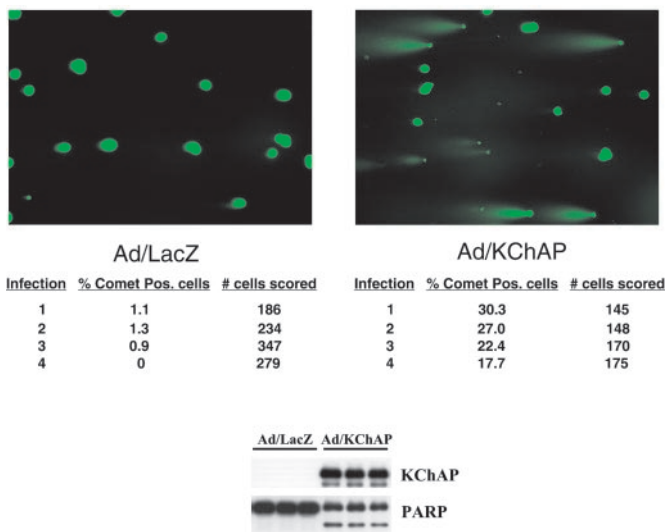
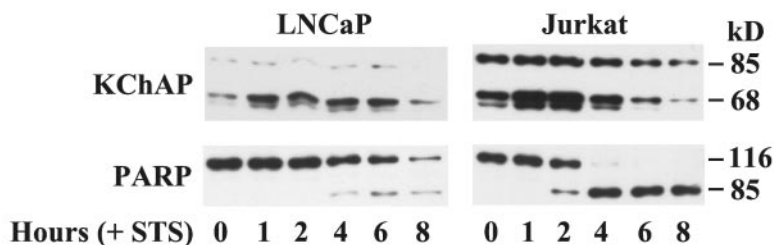


FIG. 3. KChAP overexpression produces DNA degradation and PARP cleavage in LNCaP cells. *A*, COMET assay to detect DNA degradation in LNCaP cells 3 days postinfection with Ad/LacZ or Ad/KChAP (MOI = 100). Cells were counted from four separate infections. An example of a field of cells examined for each type of infection is shown in the upper panels. Quantitation of each infection is presented below. An average of 0.8% of Ad/LacZ-infected cells were COMET-positive compared with an average of 24.4% of Ad/KChAP-infected cells ($p < 0.001$). *B*, Western blot of overexpressed KChAP (detected with 088 antibody) and PARP cleavage in LNCaP lysates prepared from cells as described for *A*. Each lane represents lysate from a separate batch of infected cells.

DNA degradation and PARP cleavage apparent 3 days after infection.

KChAP Overexpression Increases p53 Levels and p53-Serine 15 Phosphorylation—p53, a tumor suppressor protein mutated in about 50% of all human cancers, is able to induce apoptosis

as well as produce cell cycle (G_1) arrest (reviewed in Ref. 21). PIASy and PIAS1 have both been shown to interact with p53 but with differential effects on the ability of p53 to stimulate transcription (15, 19). We asked whether KChAP also interacted with p53 by using yeast two-hybrid analysis. Murine p53 (residues 90–390), with the transactivation domain removed, was found to interact with KChAP (Fig. 4A, left panel). The 98-amino acid fragment of KChAP, KChAP-M, which interacts with Kv channel NH_2 termini in yeast two-hybrid assays (8), also interacted with p53 (Fig. 4A, right). Further truncation of p53 revealed that the carboxyl-terminal 100 residues of p53 (p53CT; Val²⁹⁰–Asp³⁹⁰) were sufficient for interaction with KChAP. p53 is a functional homotetramer, and the tetramerization domain has been localized to the COOH terminus (22). The p53 carboxyl terminus (p53CT) interacts with itself in yeast two-hybrid assays (Fig. 4A, right). To further localize the sites of KChAP interaction in p53, we constructed a 28-amino acid fragment (Phe³²⁴–Thr³⁵²) from the p53 carboxyl terminus that encompassed the tetramerization domain. This fragment interacted with itself as well as KChAP (Fig. 4A). Deletion of 10 residues from the NH_2 terminus of this domain (Phe³³⁴–Thr³⁵²) eliminated self-interaction as well as interaction with KChAP. Thus, KChAP is also able to interact with p53, and the assembly domain of p53 appears to be critical for this interaction.

We next asked how overexpression of KChAP affected endogenous p53 in LNCaP cells. LNCaP cells have wild-type p53 (23), and low endogenous levels are maintained through a complex set of regulatory mechanisms. Since wild-type p53 can produce apoptosis in many cell types, we examined Ad/GFP- and Ad/KChAP-infected LNCaP lysates for p53 levels. Western blotting for total p53 protein with the DO1 antibody showed an increased amount in KChAP-overexpressing cells 3 days postinfection (Fig. 4B). The increased p53 levels were coincident with an increase in the reactivity of an antibody specific for p53 phosphorylated on serine 15. Phosphorylation at serine

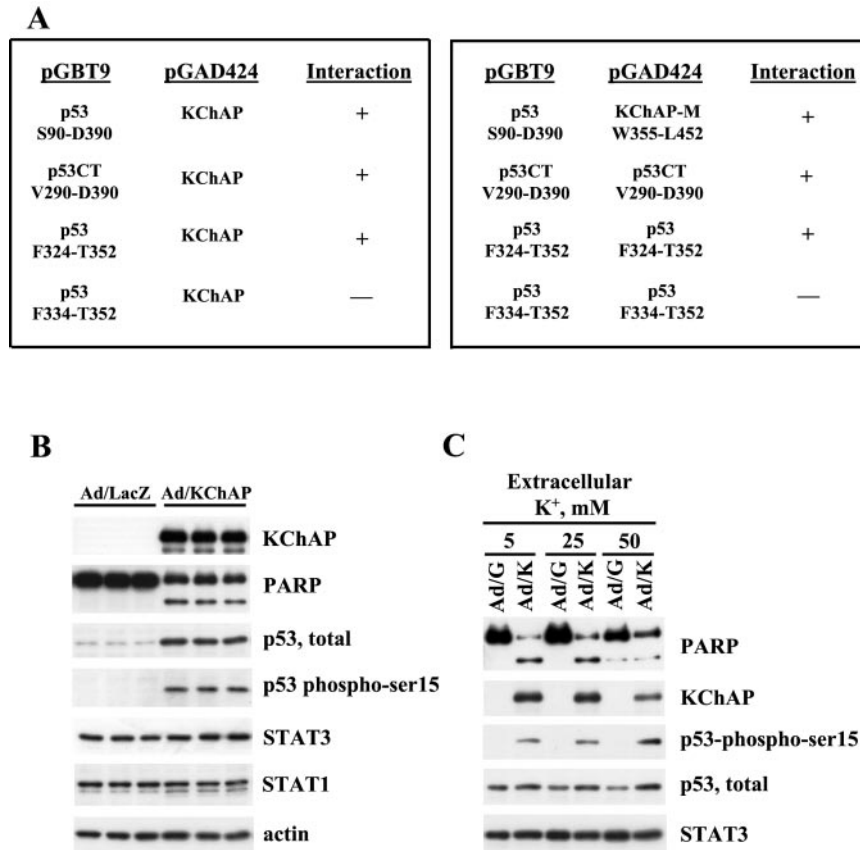


FIG. 4. KChAP overexpression increases p53 levels and p53-serine 15 phosphorylation in LNCaP cells. *A*, yeast two-hybrid analysis of KChAP interaction with p53. Pairwise combinations of KChAP with murine p53 fragments were tested for interaction after transformation into the *Y190* host strain (*left panel*). p53 fragments were tested for self-interaction (*right panel*). +, blue color development in a β -galactosidase filter lift assay within 4 h; —, lack of color development within this period. All constructs were checked for nonspecific activation of the *lacZ* reporter gene before use in these experiments (by cotransformation with the corresponding empty vector) and were negative. *B*, Western blot analysis of LNCaP cell lysates prepared 3 days after infection with Ad/KChAP or Ad/LacZ viruses (MOI of 100). Results are shown from triplicate infections. The KChAP 088 antibody reacts only with overexpressed, not endogenous, KChAP. Note that KChAP overexpression is correlated with an increase in total p53 levels (detected with the DO1 antibody) as well as phosphorylation of p53 serine 15. STAT3 and STAT1 levels are not changed. Actin is included as a loading control. *C*, LNCaP cells were infected with Ad/GFP (Ad/G) or Ad/KChAP (Ad/K) (MOI = 100) in the presence of medium in which extracellular K⁺ was altered (5, 25, or 50 mM) (see “Experimental Procedures” for details of media preparation). Lysates were prepared 72 h postinfection and examined by Western blotting for PARP, overexpressed KChAP (088 antibody), p53-phosphoserine 15, total p53 (DO1 antibody), and STAT3. STAT3 served as the loading control.

15 in p53 has been shown to have several functional consequences: 1) increased stability of p53 by prevention of binding to the regulatory protein MDM2, thus reducing ubiquitination and proteosomal degradation (24), and 2) activation of p53 as a transcription factor (25). We also examined the level of STAT proteins, since several members of the PIAS family have been shown to interact with STATs. No changes were detected in either STAT1 or STAT3 levels. These observations suggest that part of the proapoptotic effects of KChAP may be exerted through the up-regulation and activation of p53.

Since KChAP increases K⁺ efflux as well as activation of p53 and apoptosis in LNCaP cells, we next asked whether these three events are interdependent (*i.e.* is K⁺ loss required for KChAP-mediated p53 activation and apoptosis?). K⁺ efflux was blocked by incubating cells in media with high extracellular K⁺. Cells were infected with Ad/GFP or Ad/KChAP in medium with increasing concentrations of K⁺ (from 5 to 50) and maintained for 72 h prior to lysis. Fig. 4C shows that apoptosis, detected by PARP cleavage, is largely blocked in cells bathed in 50 mM K⁺. There is a small, basal level of PARP cleavage apparent in GFP-expressing cells in 50 mM K⁺, which is not accentuated in KChAP-expressing cells. Although KChAP-induced apoptosis is blocked in high extracellular K⁺, phosphorylation of p53 on serine 15 still occurs. Therefore, K⁺ efflux, although required for apoptosis, is not required for p53 activation.

KChAP Produces G₀/G₁ Cell Cycle Arrest—When p53 is activated as a transcription factor, one of its major targets is the cell cycle arrest protein, p21, and increased p21 expression has been linked to cell cycle arrest at G₀/G₁ (26). We examined the expression of p21 in Ad/KChAP-infected LNCaP cells harvested 24, 48, and 72 h postinfection. As shown in Fig. 5A, a dramatic increase in p21 levels was detected by Western blotting as early as 24 h postinfection. This increased expression was maintained at 48 and 72 h after infection and was coincident with elevated p53 levels observed at 24, 48, and 72 h in KChAP-overexpressing cells. Since elevated p21 would be expected to produce G₀/G₁ arrest, we examined the expression of a cell cycle marker protein, retinoblastoma (Rb). Rb exhibits cell cycle-specific phosphorylation (27); in G₀/G₁ cells, Rb is hypophosphorylated and migrates more rapidly on SDS-PAGE, providing a useful marker for cell cycle arrest. In GFP-expressing cells, two forms of Rb are detected: an upper, hyperphosphorylated form and a lower, hypophosphorylated form (Fig. 5A). In KChAP-expressing cells, only the lower, hypophosphorylated form is detected. This is seen as early as 24 h postinfection and is maintained throughout the assay period. In Fig. 5B, we examined the expression of several other cyclins as cell cycle markers. Cyclins A and B are mitotic cyclins whose levels decrease during G₀/G₁ (28). In KChAP-infected LNCaP cells, the levels of both cyclins A and B fall dramatically, consistent

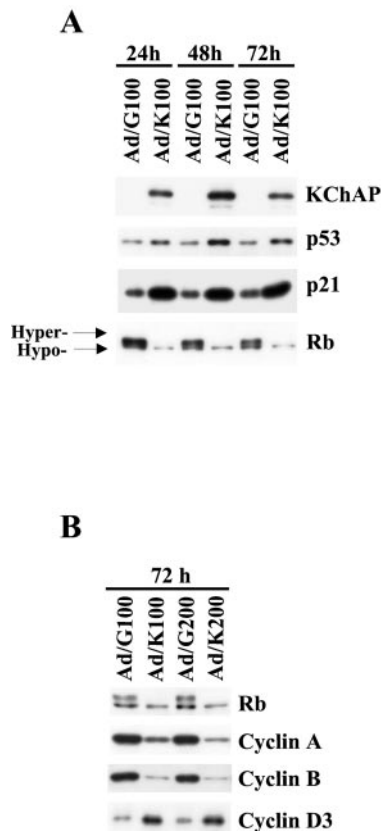


FIG. 5. KChAP produces G_0/G_1 arrest in LNCaP cells. *A*, Western blot analysis of LNCaP lysates infected either with Ad/GFP or Ad/KChAP at an MOI of 100. Cells were harvested 24, 48, or 72 h postinfection. Overexpressed KChAP was detected by the 088 antibody, and total p53 was detected by the DO-1 monoclonal antibody. Note that the levels of p21, a transcriptional target of p53 and an inducer of G_0/G_1 arrest are up in KChAP-infected cells as early as 24 h postinfection. G_0/G_1 arrest is confirmed by the pattern of Rb (retinoblastoma protein) staining as the hypophosphorylated form predominates at this stage. *B*, Western blot analysis of cyclins confirms the G_0/G_1 arrest mediated by KChAP in LNCaP cells. LNCaP cells infected with Ad/GFP or Ad/KChAP at two different MOI, 100 and 200, were examined 72 h postinfection. Rb expression confirmed G_0/G_1 arrest as seen in *A*. Consistent with this observation, the levels of two mitotic cyclins A and B were significantly decreased, whereas the level of cyclin D3, a protein predominating in G_1 , was increased.

with G_0/G_1 arrest. Conversely, a cyclin up-regulated during G_1 (cyclin D3) (29) is expressed at higher levels in KChAP-overexpressing cells. Thus, Western blotting of KChAP-infected cell lysates with cell cycle markers indicates that KChAP produces cell cycle arrest at G_0/G_1 prior to the appearance of apoptosis.

Cell cycle arrest and apoptosis induced by KChAP were also examined by flow cytometry of infected cells. Ad/GFP and Ad/KChAP-infected cells were fixed either 24 or 72 h after infection, and DNA content was assessed by propidium iodide staining. Cells were classified as either DAB (subdiploid), G_0/G_1 (diploid), S (intermediate), or G_2/M (tetraploid). A comparison of the distribution of LNCaP cells after GFP *versus* KChAP overexpression for 24 h showed an increase in the population of G_0/G_1 cells and a decrease in the number of S phase cells among the KChAP-infected group (Fig. 6A, *left panels*). A decrease in the number of S phase cells is consistent with G_0/G_1 arrest, since cells are able to exit S phase but no cells are able to enter from G_0/G_1 . The data are plotted in Fig. 6B (*left panel*) as the percentage of cells in each population. The percentage of cells in G_0/G_1 increases from 62% in GFP-expressing cells to 78% in KChAP-overexpressing cells, while the S phase population drops from 18% in GFP cells to 1% in KChAP cells. When

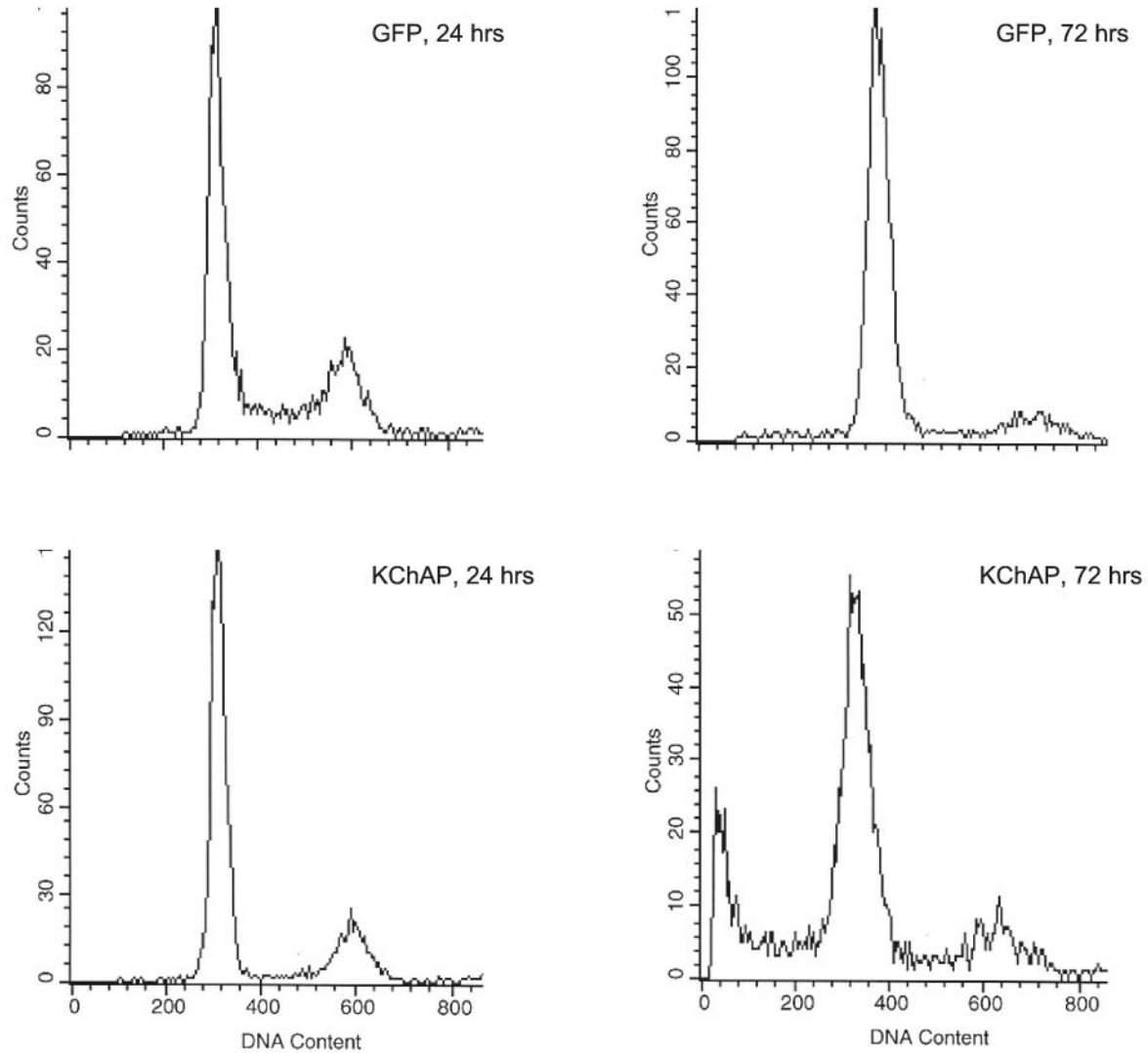
assayed 72 h after infection, there is a dramatic increase in the number of DAB cells in the KChAP-expressing group (5% in GFP cells and 20% in KChAP cells; Fig. 6, *A and B, right panels*). This group of cells with subdiploid DNA content would consist of apoptotic cells with fragmented DNA. Taken together, these data reflect the temporal pattern of the effects of KChAP on LNCaP cells. An early event (within 24 h after introduction of KChAP cDNA) is the arrest of cells in G_0/G_1 . The induction of apoptosis is detected 72 h after Ad/KChAP infection.

Wild-type p53 Is Not Required for KChAP-mediated Apoptosis—LNCaP cells possess wild-type p53. As we have shown, overexpression of KChAP in these cells produces increased steady-state levels of p53 as well as phosphorylation of p53 on serine 15. Perhaps the growth arrest and apoptosis that we observe is mediated via the activation of p53 as a transcription factor. To determine whether wild-type p53 is essential for KChAP effects, we tested the effects of KChAP in a cell line with mutant p53. The prostate cancer cell line, DU145, has p53 with several point mutations rendering it nonfunctional as a transcription factor (23). DU145 cells were infected with Ad/GFP or Ad/KChAP at two different MOI (200 and 400), and lysates were prepared 72 h after infection. Greater than 95% of the cells were infected in these experiments as determined by GFP fluorescence, and most of the KChAP-infected cells were floating by day 3 (data not shown). Western blotting shows significant PARP cleavage in DU145 cells infected with Ad/KChAP compared with control, Ad/GFP-infected cells (Fig. 7). Steady-state p53 levels are already high in DU145 cells, as is often seen when p53 is mutated, and those levels do not increase with KChAP overexpression. The phosphorylation of p53 on serine 15 is still increased in KChAP-overexpressing cells, however. Unlike LNCaP cells, there was no up-regulation of p21 evident from Western blots in KChAP-overexpressing DU145 cells (data not shown), confirming that p53 is not an active transcription factor in DU145 cells. Furthermore, flow cytometry of infected DU145 cells showed that the G_0/G_1 arrest that was apparent in KChAP-overexpressing LNCaP cells was absent from DU145 cells (data not shown). Taken together, these results suggest that wild-type p53 may be involved in KChAP-mediated G_0/G_1 arrest but is not required for apoptosis.

KChAP Prevents in Vivo Growth of Subcutaneous Implants of Human Prostate Cancer Cells—We have shown that KChAP is a potent inducer of apoptosis in cell lines with diverse p53 status. To assess its potential usefulness as an anti-cancer agent, we created subcutaneous tumors in nude mice by injecting either DU145 or LNCaP cells into the flank area. DU145 cells, mixed with Matrigel, formed established tumors in the flanks of nude mice in about 2 weeks. Once tumors were established, Ad/KChAP was injected directly into the tumors every 48–72 h for a total of nine injections over a period of 19 days. Two batches of control tumors were injected with either PBS or Ad/GFP. As shown in Fig. 8A, injection of Ad/KChAP significantly suppressed the growth of DU145 tumors compared with Ad/GFP or PBS treatments. In the animals treated with Ad/KChAP, the mean tumor volume was 81 mm³ after 19 days ($n = 8$). In contrast, the mean tumor volume reached 492 mm³ in the Ad/GFP-treated group ($n = 8$) and 716 mm³ in the PBS-injected controls ($n = 10$). At the conclusion of the treatment period, mice in the Ad/KChAP-treated group were active and appeared normal in contrast to the mice in the other two groups, which had difficulty moving because of the tumor burden and appeared ill.

Tumors from each of the three treatment groups were harvested 2 days after the last injection and processed for immu-

A



B

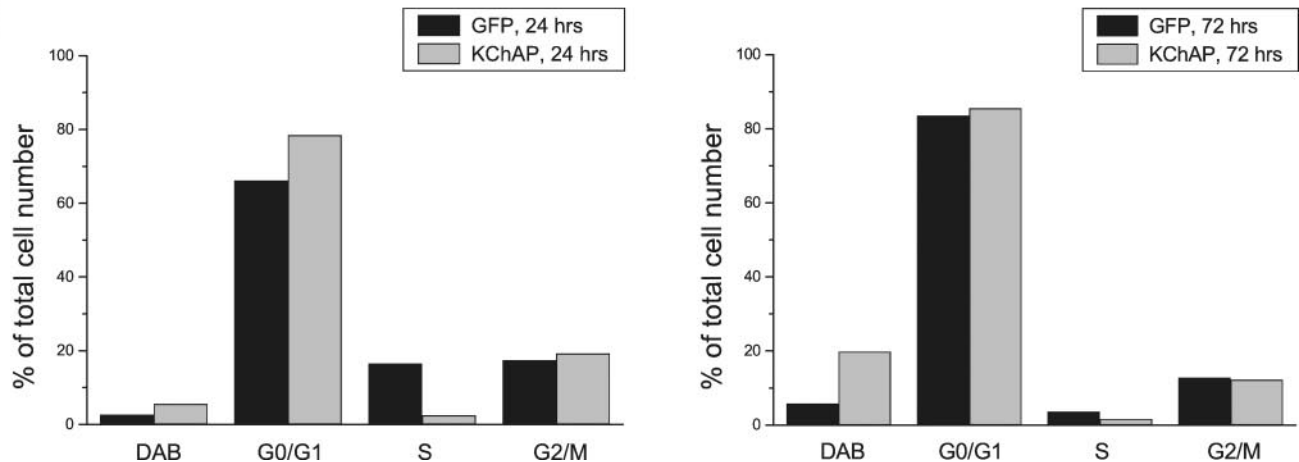


FIG. 6. **Flow cytometry analysis of effects of KChAP on LNCaP cells.** A, LNCaP cells infected with Ad/GFP or Ad/KChAP (both at MOI = 100) were fixed in cold 70% ethanol 24 h (left) or 72 h (right) after infection and stained with propidium iodide. Ten thousand cells from each sample were analyzed using FACScan as detailed under "Experimental Procedures." The x axis shows propidium iodide intensity, representing DNA content, and the y axis shows the number of events, representing cell numbers. B, histogram of cell cycle distribution. G₀/G₁, S, and G₂/M phases are indicated. The sub-G₀/G₁ (DAB) population represents apoptotic cells. The data shown are representative of three independent experiments.

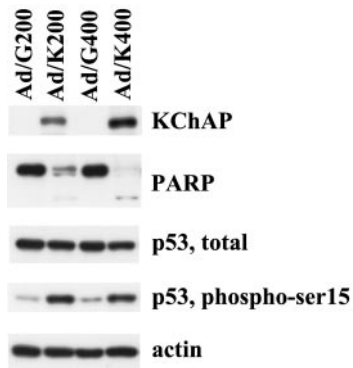


FIG. 7. KChAP induces apoptosis in p53 mutant DU145 cells. Western blots of lysates prepared 72 h postinfection from DU145 cells infected with either Ad/GFP or Ad/KChAP at two different MOI, 200 and 400. Overexpressed KChAP was detected with the 088 antibody. The PARP antibody detected both the 116-kDa intact protein as well as the 85-kDa cleavage product. Steady-state p53 levels were detected with the DO1 monoclonal antibody, and the phosphorylation state of p53-serine 15 was assessed with a specific polyclonal antibody. Actin was included as a loading control.

nohistochemistry. When dissected, Ad/KChAP-treated tumors were all localized subcutaneously with clear boundaries, while most tumors from the two control groups were found to penetrate into adjacent tissues and organs and had a well established blood supply. Sections were stained with KChAP antibody 088 to detect overexpressed KChAP, and parallel sections were assayed for TUNEL-positive cells (*i.e.* apoptotic cells with fragmented DNA). Staining with the KChAP 088 antibody was seen in many cells from tumors injected with Ad/KChAP with very little background staining in tumors treated with either Ad/GFP or PBS (Fig. 8B, right panels). We have seen previously that the 088 antibody does not stain either DU145 or LNCaP cells in culture.² As predicted from our *in vitro* data, overexpression of KChAP was accompanied by apoptosis in the infected tumor cells as the comparison of TUNEL-positive cells from each of the three treatment groups showed (Fig. 8B, left panels). A low background level of TUNEL-positive cells was seen in Ad/GFP- and PBS-treated tumors with a significant enhancement in the number of TUNEL-positive or apoptotic cells seen in KChAP-overexpressing tumors.

We also tested LNCaP cells in nude mice, but, in contrast to DU145 cells, LNCaP cells did not generate a sufficient number of large tumors, even 5 weeks after injection of cells, to do a complete experiment. However, in the few large tumors that were produced, we observed similar results with Ad/KChAP injection. Overexpressed KChAP shrunk LNCaP tumors to half their original size, whereas Ad/GFP- or PBS-treated tumors tripled tumor volume in a 5-week period (data not shown). Immunohistological examination of LNCaP-derived tumor sections showed 088 antibody-positive staining that correlated with increased apoptosis and TUNEL-positive cells (data not shown).

DISCUSSION

We have shown that infection of a recombinant adenovirus overexpressing KChAP/PIAS3 β (Ad/KChAP) in LNCaP and DU145 prostate cancer cells produces apoptosis, and direct injection of Ad/KChAP into xenografts of LNCaP and DU145 cells in nude mice suppresses tumor growth. These data support a link between overexpression of KChAP/PIAS3 β and the increased K⁺ efflux that results during apoptotic volume decrease. Increased K⁺ efflux from Ad/KChAP-infected LNCaP

cells was shown by Rb⁺ flux measurements, and decreased intracellular K⁺ and cell shrinkage were demonstrated by flow cytometry. Apoptosis in Ad/KChAP-infected LNCaP cells was blocked by high extracellular K⁺, indicating that KChAP-enhanced K⁺ efflux is critical for apoptosis. The identity of the K⁺ channel(s) that carries the increased outward current has not yet been determined. We attempted to infect cells in the presence of K⁺ channel blockers such as 4-AP, TEA, and quinidine to assess the effects on apoptosis, but these experiments were unsuccessful, since the drugs also interfered with viral infection. LNCaP cells are known, however, to possess several outward K⁺ currents including voltage-gated delayed rectifier channels (30, 31) as well as several two-pore K⁺ channel-like currents.² Recently, two-pore K⁺ channels were proposed as candidates for mediating apoptotic volume decrease (32). Future experiments should reveal both the K⁺ channels mediating apoptotic volume decrease in LNCaP cells and the role of KChAP in modulating these channels. With the results presented here, we propose that KChAP is an attractive candidate for the long sought after mediator of apoptotic volume decrease.

KChAP/PIAS3 β not only affects K⁺ channels but, as a member of the PIAS family, interacts with a variety of transcription factors. We have found that KChAP/PIAS3 β , like other members of the PIAS family, binds to p53 and alters its transcriptional activity. Interestingly, the same KChAP domain that binds to Kv channel NH₂ termini (*i.e.* the 98-amino acid M-fragment) (8) also interacts with p53 in yeast two-hybrid experiments. We have identified a 28-residue fragment from the COOH terminus of p53, consisting of the tetramerization domain, which is sufficient for interaction with KChAP. This result is consistent with a recent report indicating that PIAS1 also interacts with the tetramerization domain of p53 (19).

Our data show that KChAP/PIAS3 β activates p53 in LNCaP cells. When p53 is activated as a transcription factor, the cell cycle arrest protein gene, p21, is a target. We see both increased total p53 and p21 levels in Ad/KChAP-infected LNCaP cells, suggesting an activation of p53. PIAS1 has been shown to interact with p53 and activate its transcriptional activity (19). Another PIAS family member, PIASy, interacts with p53 but depresses rather than enhances its activity as a transcription factor (15), suggesting distinct functions of individual PIAS proteins.

One mechanism whereby PIAS proteins might activate p53 is suggested by our observation of increased p53 phosphorylation on serine 15 in Ad/KChAP-infected cells. Phosphorylation of this residue has been shown previously to correlate with increased stability of p53 as well as increased transcriptional activity (24, 25). KChAP-induced loss of K⁺ is not required for p53 activation, since serine 15 phosphorylation is also detected in cells bathed in high extracellular K⁺. This effect is distinct from caspase activation, which requires loss of intracellular K⁺. It is not known whether other PIAS proteins induce the same modification in p53 or how KChAP produces this post-translational modification. Several kinases have been implicated in the phosphorylation of p53 serine 15 including ATM, ATR, and c-Jun N-terminal kinase (reviewed in Ref. 33). Interestingly, PIAS1 has been shown to induce apoptosis in U2OS cells via activation of c-Jun N-terminal kinase (34), suggesting a possible link between c-Jun N-terminal kinase and p53 phosphorylation. We have observed activation of c-Jun N-terminal kinase as well as p38 and extracellular signal-regulated kinase 1 and 2 kinases in Ad/KChAP-infected LNCaP cells.²

The pleiotropic nature of PIAS protein action as well as the variety of binding partners identified thus far must now be considered in light of the recent implication of PIAS proteins as SUMO-1 E3 ligases. PIAS1 has been shown to catalyze the

² B. A. Wible, L. Wang, Y. A. Kuryshev, A. Basu, S. Haldar, and A. M. Brown, unpublished observations.

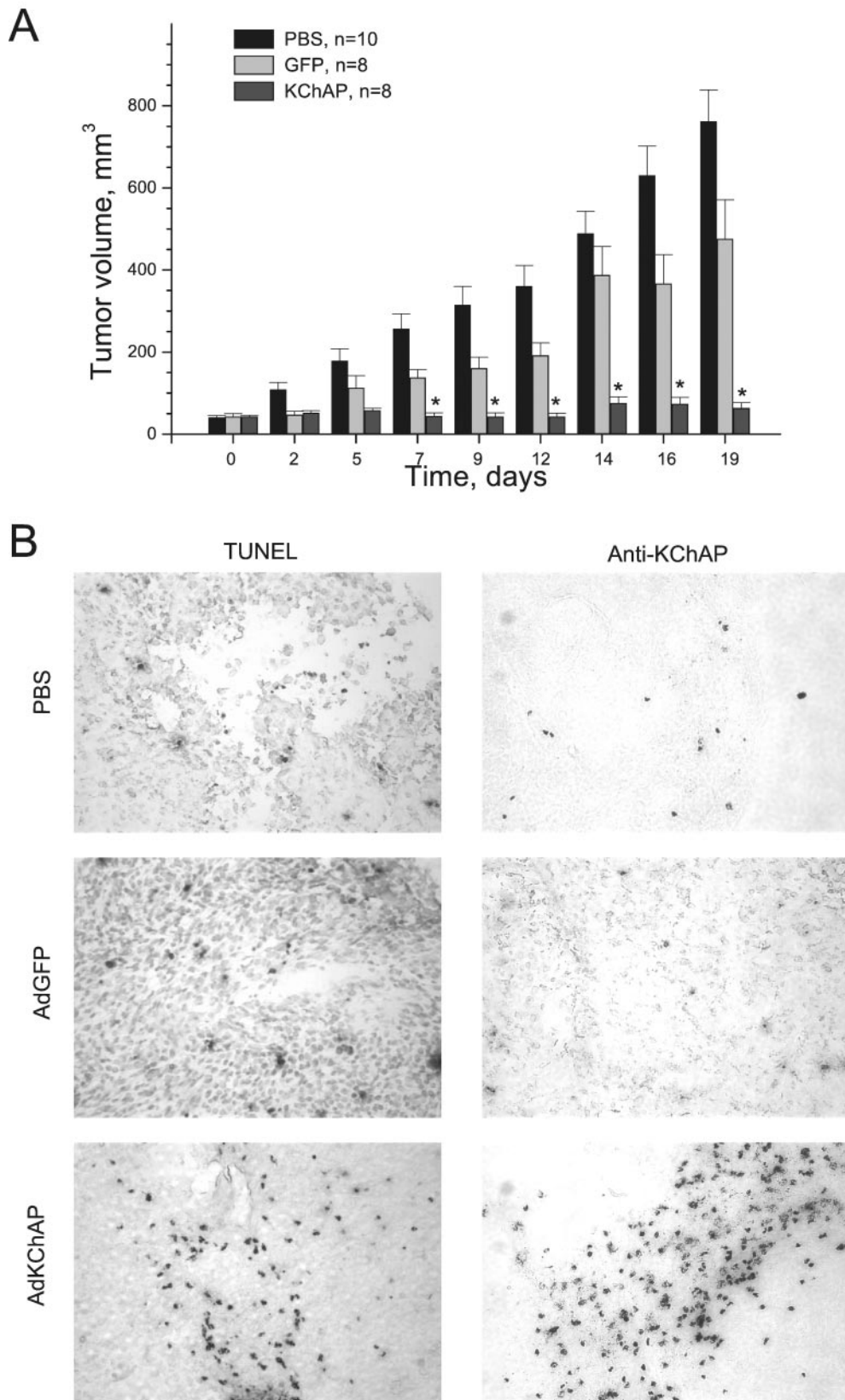


FIG. 8. Ad/KChAP inhibits growth of DU145 tumor xenografts in nude mice. *A*, comparison of average DU145 tumor sizes among three treatment groups: PBS, Ad/GFP, Ad/KChAP. DU145 cells injected into the flanks of nude mice were allowed to reach a volume of ~ 50 mm³, after which the tumors were injected every 48–72 h with either PBS, Ad/GFP, or Ad/KChAP for a total of nine injections over a 19-day period. By day 7, the tumor volume of Ad/KChAP-injected tumors was significantly less than either PBS or Ad/GFP-injected tumors (*, $p < 0.01$). There was no significant difference in tumor size between the PBS and Ad/GFP control groups. *B*, KChAP immunohistochemistry and TUNEL assay in tumor sections from animals sacrificed 2 days after the last injection (*i.e.* day 21 after the start of treatment). KChAP overexpression was detected in treated tumor sections with the KChAP 088 antibody and colorimetric detection (*right panels*), and corresponding apoptosis was detected with the TUNEL assay (*left panels*).

sumoylation (*i.e.* covalent attachment of the small ubiquitin-like modifier protein, SUMO-1) of p53 in mammalian cells (35), and interestingly, sumoylation was previously reported to increase the transcriptional activity of p53 (36, 37). In *Saccharomyces cerevisiae*, the PIAS homolog, Siz1, has been shown to act as an E3-like factor for SUMO-1 conjugation to the septins, a process required for yeast budding (38–40). In addition, the transcriptional activity of the androgen receptor, another PIAS-binding protein, can be modified by sumoylation (41), although it is not known whether PIAS proteins mediate this process. It will be important to determine the role that sumoylation plays in the involvement of PIAS proteins with all binding partners, including the interaction of KChAP/PIAS3 β with K⁺ channels, to ultimately produce apoptosis.

The proapoptotic properties of KChAP/PIAS3 β overexpression suggested that it might present a novel method of anti-tumor therapy. We tested this idea by direct injection of Ad/KChAP adenovirus into xenograft tumors of DU145 and LNCaP cells in nude mice and observed a striking growth inhibition in tumors derived from both cell types. Importantly, wild-type p53 is not required for KChAP/PIAS3 β -mediated apoptosis, since LNCaP and DU145 cells express wild-type and mutant p53, respectively. KChAP induction of p53-independent apoptosis may be important therapeutically, since 50% of human tumors express mutant p53. There is currently great interest in developing novel apoptosis-based anti-cancer treatments (42), and our data suggest that KChAP/PIAS3 β may provide a novel molecule for therapeutic development.

Acknowledgments—We thank H. Liu and M. Mohan for technical assistance and Dr. T. Scarpa for access to the flame atomic absorption spectrometer at Case Western Reserve University.

REFERENCES

- Yu, S. P., Canzoniero, L., and Choi, D. W. (2001) *Curr. Opin. Cell Biol.* **13**, 405–411
- Yu, S. P., Yeh, C. H., Sensi, S. L., Gwag, B. J., Canzoniero, L. M., Farhangrazi, Z. S., Ying, H. S., Tian, M., Dugan, L. L., and Choi, D. W. (1997) *Science* **278**, 114–117
- Yu, S. P., Yeh, C. H., Gottron, F., Wang, X., Grabb, M. C., and Choi, D. W. (1999) *J. Neurochem.* **73**, 933–941
- Krick, S., Platoshyn, O., Sweeney, M., Kim, H., and Yuan, J. X. (2001) *Am. J. Physiol.* **280**, C970–C979
- Krick, S., Platoshyn, O., McDaniel, S. S., Rubin, L. J., and Yuan, J. X. (2001) *Am. J. Physiol.* **281**, L887–L894
- Hughes, F. M., and Cidowski, J. (1999) *Adv. Enzyme Reg.* **39**, 157–171
- Wible, B. A., Yang, Q., Kuryshev, Y. A., Accili, E. A., and Brown, A. M. (1998) *J. Biol. Chem.* **273**, 11745–11751
- Kuryshev, Y. A., Gudiz, T. I., Brown, A. M., and Wible, B. A. (2000) *Am. J. Physiol.* **278**, C931–C941
- Kuryshev, Y. A., Wible, B. A., Gudiz, T. I., Ramirez, A. N., and Brown, A. M. (2001) *Am. J. Physiol.* **281**, C290–C299
- Chung, C. D., Liao, J., Liu, B., Rao, X., Jay, P., Berta, P., and Shuai, K. (1997) *Science* **278**, 1803–1805
- Valdez, B. C., Henning, D., Perlaky, L., Busch, R. K., and Busch, H. (1997) *Biochem. Biophys. Res. Commun.* **234**, 335–340
- Liu, B., Liao, J., Rao, X., Kushner, S. A., Chung, C. D., Chang, D. D., and Shuai, K. (1998) *Proc. Natl. Acad. Sci. U. S. A.* **95**, 10626–10631
- Moilanen, A. M., Karvonen, U., Poukka, H., Yan, W., Toppari, J., Janne, O. A., and Palvimo, J. J. (1999) *J. Biol. Chem.* **274**, 3700–3704
- Wu, L., Wu, H., Ma, L., Sangiorgi, F., Wu, N., Bell, J. R., Lyons, G. E., and Maxson, R. (1997) *Mech. Dev.* **65**, 3–17
- Nelson, V., Davis, G. E., and Maxwell, S. A. (2001) *Apoptosis* **6**, 221–234
- Kotaja, N., Aittomaki, S., Silvennoinen, O., Palvimo, J. J., and Janne, O. A. (2000) *Mol. Endocrinol.* **14**, 1986–2000
- Tan, J., Hall, S. H., Hamil, K. G., Grossman, G., Petrusz, P., Liao, J., Shuai, K., and French, F. S. (2000) *Mol. Endocrinol.* **14**, 14–26
- Gross, M., Liu, B., Tan, J., French, F. S., Carey, M., and Shuai, K. (2001) *Oncogene* **20**, 3880–3887
- Megidish, T., Xu, J. H., and Xu, C. W. (2002) *J. Biol. Chem.* **277**, 8255–8259
- Terstappen, G. C. (1999) *Anal. Biochem.* **272**, 149–155
- Bargonetti, J., and Manfredi, J. J. (2002) *Curr. Opin. Oncol.* **14**, 86–91
- Chene, P. (2001) *Oncogene* **20**, 2611–2617
- Isaacs, W. B., Carter, B. S., and Ewing, C. M. (1991) *Cancer Res.* **51**, 4716–4720
- Shieh, S. Y., Ikeda, M., Taya, Y., and Prives, C. (1997) *Cell* **91**, 325–334
- Dumaz, N., and Meek, D. W. (1999) *EMBO J.* **18**, 7002–7010
- Deng, C., Zhang, P., Harper, J. W., Elledge, S. J., and Leder, P. (1995) *Cell* **82**, 675–684
- Weinberg, R. A. (1995) *Cell* **81**, 323–330
- Pines, J., and Hunter, T. (1994) *EMBO J.* **13**, 3772–3781
- Hunter, T., and Pines, J. (1995) *Cell* **79**, 573–582
- Skyrma, R. N., Prevarskaya, N. B., Dufy-Barbe, L., Odess, M. F., Audin, J., and Dufy, B. (1997) *Prostate* **33**, 112–122
- Laniado, M. E., Fraser, S. P., and Djamgoz, M. B. (2001) *Prostate* **46**, 262–274
- Trimarchi, J. R., Liu, L., Smith, P. J. S., and Keefe, D. L. (2002) *Am. J. Physiol.* **282**, C588–C594
- Appella, E., and Anderson, C. W. (2001) *Eur. J. Biochem.* **268**, 2764–2772
- Liu, B., and Shuai, K. (2001) *J. Biol. Chem.* **276**, 36624–36631
- Kahyo, T., Nishida, T., and Yasuda, H. (2001) *Mol. Cell* **8**, 713–718
- Gostissa, M., Hengstermann, A., Fogal, V., Sandy, P., Schwarz, S. E., Scheffner, M., and Del Sal, G. (1999) *EMBO J.* **18**, 6462–6471
- Rodriguez, M. S., Desterro, J. M., Lain, S., Midle, C. A., Lane, D. P., and Hay, R. T. (1999) *EMBO J.* **18**, 6455–6461
- Johnson, E. S., and Gupta, A. A. (2001) *Cell* **106**, 735–744
- Takahashi, Y., Toh-e, A., and Kikuchi, Y. (2001) *Gene (Amst.)* **275**, 223–231
- Takahashi, Y., Kahyo, T., Toh-e, A., Yasuda, H., and Kikuchi, Y. (2001) *J. Biol. Chem.* **276**, 48973–48977
- Poukka, H., Karvonen, U., Janne, O. A., and Palvimo, J. J. (2000) *Proc. Natl. Acad. Sci. U. S. A.* **97**, 14145–14150
- Reed, J. C. (2002) *Nat. Rev. Drug Discovery* **1**, 111–121